Received: 21 July 2024 | Revised: 25 October 2024 | Accepted: 16 November 2024

DOI: 10.1111/jne.13476

ORIGINAL ARTICLE

Journal of Neuroendocrinology WILEY

From silence to song: Testosterone triggers extensive transcriptional changes in the female canary HVC

Meng-Ching Ko[1] | Carolina Frankl-Vilches[1] | Antje Bakker[1] | Nina Sohnius-Wilhelmi[1] | Pepe Alcami[1,2] | Manfred Gahr[1]

[1]Department of Behavioural Neurobiology, Max Planck Institute for Biological Intelligence, Seewiesen, Germany

[2]Division of Neurobiology, Faculty of Biology, Ludwig-Maximilians-University Munich, Planegg, Germany

Correspondence
Meng-Ching Ko, Evolution of Sensory and Physiological Systems, Max Planck Institute for Biological Intelligence, Martinsried, 82152, Germany.
Email: mengching.ko@bi.mpg.de

Funding information
Max-Planck-Gesellschaft

Abstract

Seasonal song production in canaries is influenced by gonadal hormones, but the molecular mechanisms underlying testosterone-induced song development in adult female canaries, which rarely sing naturally, remain poorly understood. We explored testosterone-induced song development in adult female canaries by comparing gene regulatory networks in the song-controlling brain area HVC at multiple time points (1 h to 14 days) post-treatment with those of placebo-treated controls. Females began vocalizing within 4 days of testosterone treatment, with song complexity and HVC volume increasing progressively over 2 weeks. Rapid transcriptional changes involving 2739 genes preceded song initiation. Over 2 weeks, 9913 genes—approximately 64% of the canary's protein-coding genome—were differentially expressed, with 98% being transiently regulated. These genes are linked to various biological functions, with early changes at the cellular level and later changes affecting the nervous system level after prolonged hormone exposure. Our findings suggest that testosterone-induced song development is accompanied by extensive and dynamic transcriptional changes in the HVC, implicating widespread neuronal involvement. These changes underpin the gradual emergence of singing behavior, providing insights into the neural basis of seasonal behavioral patterns.

KEYWORDS
gene expression, HVC, plasticity, singing behavior, testosterone

1 | INTRODUCTION

Adult socio-sexual behaviors in vertebrates are critically regulated by gonadal hormones, particularly androgens and estrogens,[1–3] which fluctuate in response to environmental conditions.[4,5] These hormones can induce significant changes in brain sensitivity and structure, leading to altered neural circuit configurations that underpin seasonal behaviors. A prominent example of this phenomenon is the seasonal singing of some songbird species, which coincides with morphological changes in song-controlling brain regions.[6–10]

Androgens and estrogens exert their effects through genomic pathway, binding to their respective receptors that act as transcription factors to regulate gene expression over hours to days.[11,12] Additionally, rapid non-genomic effects can occur within seconds to minutes via, likely, yet unknown membrane-associated receptors. These membrane-initiated actions can modulate neuronal excitability and neurotransmitter release, providing a mechanism for rapid steroid influence on neural function.[13] While these hormones may affect several regions of a neural circuit, the impacted gene cascades within a specific brain region seem limited in adults.[14,15] Unraveling the

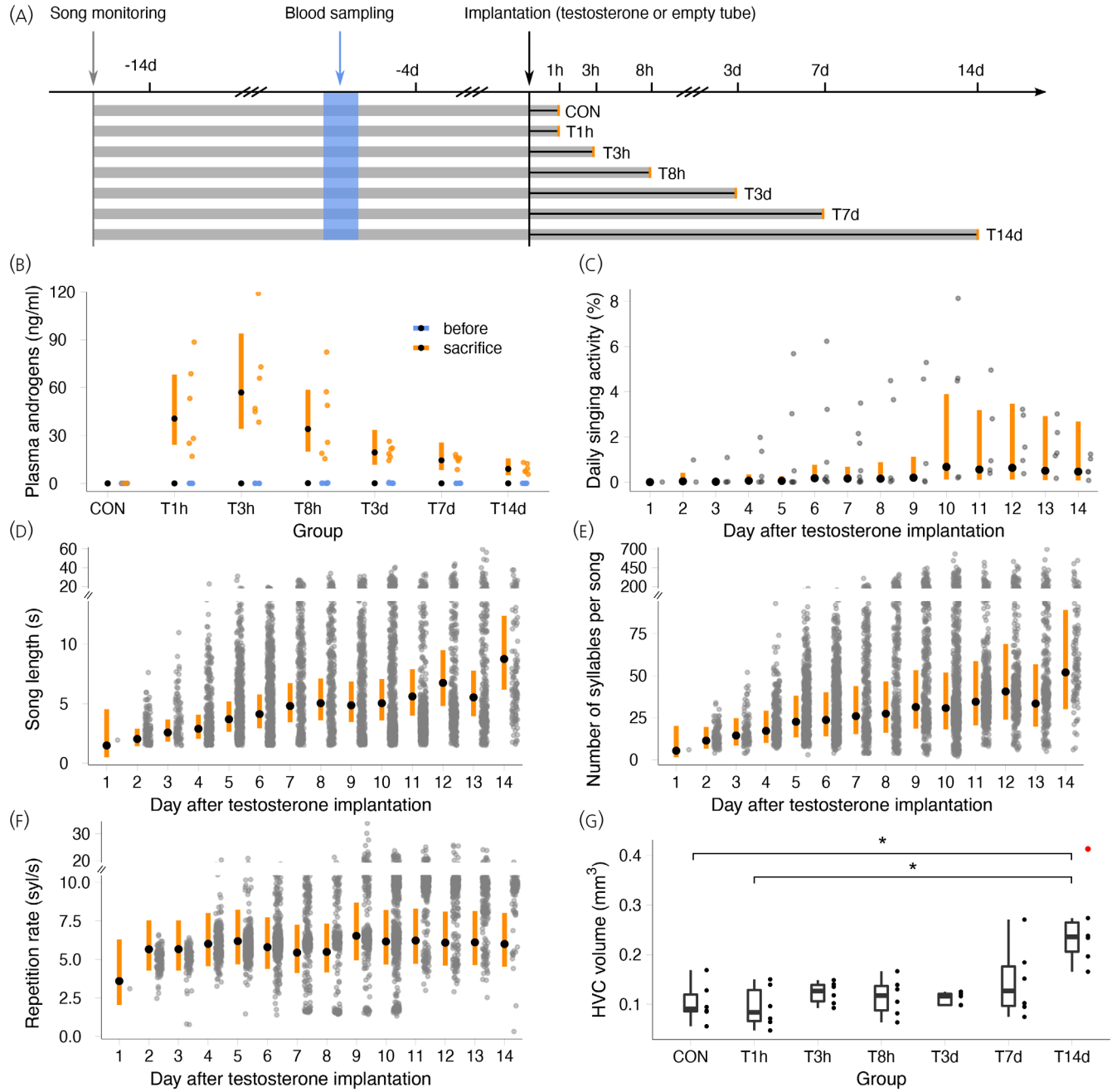

FIGURE 1 Testosterone implantation affects blood androgen levels, HVC morphology, and song syntax in adult female canaries. (A) Experimental timeline. Blood samples were collected before implantation (blue) and at sacrifice (orange). CON: control birds with empty implants; T: testosterone-treated birds for 1 h (T1h) to 14 days (T14d). (B) Testosterone significantly increased plasma androgen levels at all time points. Blue: pre-implantation; orange: post-implantation. Black dots: predicted estimates from linear mixed-effects models; orange bars: 95% credibility intervals (CrI). See Supplemental Tables 2 and 3 for the values of the linear mixed-effects models and posterior probabilities. (C) Daily singing activity (% of 9-h period) in T7d and T14d groups increased significantly twice: on days 2 and 10 (see also Figure 1; Supplemental Figure 3). Each grey dot is one bird. (D) Song length (seconds, s) in T7d and T14d groups increased daily until day 7, with further increase on day 11. (E) Number of syllables per song in T7d and T14d groups increased daily post-implantation. (F) Syllable repetition rate (syllables/second) in T7d and T14d groups increased significantly on days 2 and 9. In (D,E, F), each gray dot represents a measurement originating from one song; black dots show predicted estimates from linear mixed-effects models; orange bars indicate 95% CrI. See Supplemental Tables 2 and 3 for the estimates of the linear mixed-effects models and the posterior probabilities. (G) HVC volumes of T14d were significantly different from the control and T1h groups. Boxes: 25th/50th/75th percentiles; whiskers: values within 1.5 times IQR; red dots: outliers. *: Holm-adjusted *p*-value <0.05 (Kruskal–Wallis test followed by Dunn's post hoc test). Sample sizes of panel (B) to (G) are listed in Table 1.

TABLE 1 Experimental groups and sample sizes.

				Sample size (*n*)				
Group	Sex	Singing	Tissue sampled	Song analysis	Body weight, brain weight, plasma androgens	HVC volume	Microarray	Oviduct weight
CON	Female	No	HVC	-	6	6	5	6
T1h	Female	No	HVC	-	6	6	6	2
T3h	Female	No	HVC	-	6	6	5	2
T8h	Female	No	HVC	-	6	6	5	6
T3d	Female	No	HVC	-	6	5	6	3
T7d	Female	Yes	HVC	5	6	6	6	6
T14d	Female	Yes	HVC	6	6	6	6	6

Note: CON: control birds treated with empty implants; HVC: used as a proper name. Testosterone treatments: 1 h (h) [T1h], 3 h [T3h], 8 h [T8h], 3 days (d) [T3d], 7 d [T7d], and 14 d [T14d].

complex interplay between hormones, gene expression, brain structure, and behavior is particularly challenging when investigating behaviors that emerge slowly over time, such as the seasonal singing of canaries.[16,17]

Singing behavior in songbirds is a complex process involving intensive integration of sensory inputs and motor outputs.[18] In many North temperate species, sexually motivated singing is typically limited to males and is sensitive to testosterone and its metabolites.[19,20] The neural song control system of songbirds[18,21] is a target of testosterone due to the abundant expression of androgen and estrogen receptors.[22,23]

The nucleus HVC, a sensorimotor integration center of the song system, controls the temporal pattern of singing.[24,25] As the only song-control nucleus expressing both androgen and estrogen receptors,[26,27] the HVC is likely subject to extensive hormonal regulation at various organizational levels. Testosterone has been shown to induce angiogenesis in adult female canaries' HVC within a week,[28] increase the recruitment of new neurons,[29] and promote the growth of HVC volume.[30,31]

Female canaries (*Serinus canaria*) provide a unique model for studying testosterone-induced changes in singing behavior. Typically non-singers, these females possess the necessary underlying circuitry that can be activated by testosterone, leading to the production of male-like songs over several weeks.[32,33] This model allows for the examination of transcriptional cascades in parallel with the differentiation of the song control system and the progression of song development, without the confounding impact of fluctuating testosterone levels seen in males.

While a handful of studies documented transcriptomic changes in songbird brains after several weeks of testosterone treatment,[15,34–37] the transcriptomic effects at the onset of testosterone-driven singing and the progression of gene expression cascades associated with anatomical changes in the song control system and the development of singing behavior remain unexplored. By examining earlier time points—from as soon as 1 h after testosterone administration—we aim to capture the initial molecular events that may trigger subsequent neural plasticity and behavioral changes. Recent evidence shows that testosterone-sensitive singing behaviors can be modified within days during social interactions,[38] highlighting the importance of understanding early hormone responses. Understanding these early responses, which complement previously documented changes after weeks of testosterone exposure, is essential for elucidating how testosterone influences the brain and behavior from initial exposure through later timepoints.

In this study, we investigate both the immediate and sustained responses of HVC gene expression following testosterone treatment in adult female canaries. By selecting six specific time points—1 h (h) [T1h], 3 h [T3h], 8 h [T8h], 3 days (d) [T3d], 7 d [T7d], and 14 d [T14d]—we aim to capture the full temporal spectrum of testosterone's effects (Figure 1A,B and Table 1). Throughout these periods, we monitored vocal activity, gene expression, and neuroanatomical changes. This approach allows us to dissect the progression of gene expression cascades and link them to neural and behavioral outcomes. Contrary to our expectation of gradual gene recruitment, our results reveal an immediate and significant impact on HVC gene expression with dynamic patterns over time, affecting 9913 genes over 2 weeks, including 843 transcription factors, highlighting the extensive and rapid influence of testosterone on neural plasticity and behavior.

2 | MATERIALS AND METHODS

2.1 | Animals

Forty-two adult female common outbred domesticated canaries (*Serinus canaria*, at least 1-year-old) were used in this study (Table 1). Birds were bred in the animal facility of the Max Planck Institute for Biological Intelligence, Seewiesen, Germany. Housing and welfare adhered to the European Directives for the protection of animals used for scientific purposes (2010/63/EU), with protocols approved by the Government of Upper Bavaria (AZ-No. 55.2/54-2531-68/12). The study followed ARRIVE guidelines,[39] with a checklist provided in the manuscript.

Bird sex was confirmed by polymerase chain reaction using primers P2 and P8 for the CHD genes[40] and by post-mortem

inspection of the female reproductive system. Food and water were provided ad libitum. Six to 8 weeks before the experiment (starting no earlier than September), the light schedule was gradually adjusted to short-day conditions (light: dark = 9:15 h). After acclimation to this cycle, singing was monitored. Birds were divided into a control group and six experimental groups (Table 1). Experimental groups received testosterone implants for varying durations: 1 h (T1h), 3 h (T3h), 8 h (T8h), 3 d (T3d), 7 d (T7d), and 14 d (T14d) (see "Materials and Methods": "Testosterone implantation").

2.2 | Song monitoring

About 5% of female canaries sing spontaneously without hormone manipulation.[41] To ensure that vocal activity in our experiment was indeed triggered by testosterone implantation, birds used in this study were housed alone in sound-attenuated boxes (70 × 50 × 50 cm) and all vocalizations were recorded continuously for 2 weeks before testosterone implantation and until euthanasia. The microphone (TC20, Earthworks, Milford, NH) in each silenced box was connected to a PR8E amplifier (SM Pro Audio, Melbourne, Australia) that fed into an Edirol USB audio recording device (Edirol UA 1000, Roland, Los Angeles, CA) connected to a computer. Vocalizations were recorded at a sampling rate of 44.1 kHz and a resolution of 16 bits using Sound Analysis Pro 2011 software.[42]

2.3 | Song analysis

Song data analysis was limited to the T7d and T14d groups, as testosterone-treated birds began singing unstable subsongs on average by day 4. Nine hours of recordings were analyzed daily from day 0 until euthanasia (day 7 or 14). Data from T7d and T14d birds were combined for the first 7 d' analysis, as their songs did not differ significantly (Figure 1, Supplemental Figure 3, Supplemental Tables 2, and 3).

Analysis was performed using Multi_Channel_Analyser (MCA), a custom MATLAB program (version R2016b, MathWorks) with a graphical user interface, as previously described (Ko et al. 2020)[41] and publicly available (https://doi.org/10.5281/zenodo.1489098). MCA generates sound spectrograms using a fast Fourier transform with a sliding time window of 294 samples and 128 sample overlap, resulting in a spectrogram resolution of 150 Hz (frequency) and 3.76 ms (time).

Syllable recognition involved three steps due to background noise. First, sound segments (songs and calls) were manually selected by visual inspection. Second, song segments longer than 2 s were selected. Third, syllables within selected segments were automatically detected using MCA with parameters set to "High-pass filter" 2.0 kHz, "Threshold_wave_amplitude" 0.001, and "Threshold_syllable_freq" 50 Hz. Sounds shorter than 5 ms were removed.

We analyzed four song-level parameters (song length, number of syllables per song, syllable repetition rate, and slope coefficient α[43–45]) and four syllable-level parameters (syllable length, syllable spacing, peak frequency, and Wiener entropy).

Song length was calculated from the first syllable's start to the last syllable's end. Syllable repetition rate was defined as syllables per second. Syllable length and spacing were calculated from syllable timestamps. Peak frequency was the frequency of maximum power in the syllable spectrogram. Wiener entropy, a measure of signal noise, was log-transformed for a broader range (0 represents white noise; infinity represents pure tone).[42]

2.4 | Testosterone implantation

Custom-made testosterone implants were prepared by packing testosterone (Sigma-Aldrich, 86500, Saint Louis, MO) into 7-mm-long SilasticTM tubes (Dow Corning, Midland, MI; 1.47 mm inner diameter, 1.96 mm outer diameter, 0.23 mm thickness). Both ends were sealed with silicone elastomer (3140, Dow Corning). Implants were cleaned with 100% ethanol to remove any testosterone particles and tested for leakage by overnight immersion in ethanol; moist implants were discarded. One day before implantation, implants were incubated overnight in 0.1 M phosphate-buffered saline (PBS) to ensure immediate testosterone release upon implantation.[29]

Subcutaneous implantation began immediately after lights-on at 8:30 a.m., with a 20-min interval between each bird to account for euthanasia timing on the day of sacrifice. A small incision (approximately 5 mm in length) was made on the back of the bird over the pectoral musculature, usually on the right side, and one testosterone implant was placed subcutaneously. The skin was closed immediately by application of tissue glue. No anesthesia, analgesia, or feather removal was performed to minimize handling time and potential stress.

Control animals received empty 7-mm silicone tubes sealed with silicone elastomer. After the designated implantation period (1, 3, 8 h, 3, 7, or 14 d; Table 1), birds were euthanized with an isoflurane overdose. Body weight was recorded, and brains and oviducts were dissected, weighed, frozen on dry ice, and stored at −80°C until further use. Oviducts of 11 birds were not collected or weighed during dissection due to inadvertent omissions during sampling. At euthanasia, all testosterone implants were present and contained testosterone.

2.5 | Radioimmunoassay of plasma androgens

To confirm increased circulating androgen levels following hormone manipulation, we performed a radioimmunoassay on blood samples collected before and after testosterone implantation (Figure 1A). Approximately 100 μL of blood was collected twice from the wing vein—once around 4 d before implantation and once immediately before euthanasia, which corresponded to the end of each bird's designated treatment period (1, 3, 8 h, 3, 7, or 14 d after implantation). This approach allowed us to measure testosterone levels before and after treatment for each individual bird. Samples were collected

between 8 and 11 a.m. within 3 min to minimize handling effects.[46] Blood was centrifuged (2000 g, 10 min) to separate plasma. Testosterone in plasma were measured using a commercial antiserum to testosterone (T3-125, Endocrine Sciences, Tarzana, CA) as described by.[47] Standard curves and sample concentrations were calculated with Immunofit 3.0 (Beckman Inc., Fullerton, CA) using a four-parameter logistic curve fit and corrected for individual recoveries.

Testosterone concentrations were assayed in duplicates across four separate assays, with a mean extraction efficiency of 84.0 ± 6.8% ($N = 120$). The lower detection limits for the assays were 0.32–0.44 pg per tube, and all samples were above this limit. Intra-assay coefficients of variation for a chicken plasma pool were 4.4%, 4.1%, 9.8%, and 2.6%, and the inter-assay coefficient of variation was 4.3%. The testosterone antibody cross-reacts significantly with 5α-dihydrotestosterone (44%), so measurements include a fraction of 5α-DHT and are referred to as plasma androgen levels.

2.6 | Brain sectioning

Brains were sagittally sectioned using a cryostat (Jung CM3000, Leica, Wetzlar, Germany) to obtain both thick (40 or 50 μm) and thin (20 or 14 μm) sections in either 40 μm × 4 + 20 μm × 2 ($N = 18$) or 50 μm × 4 + 14 μm × 3 ($N = 24$) combinations. Thick sections were mounted on glass slides for microdissection and microarray analysis, providing sufficient tissue volume for RNA extraction while reducing processing time. Thin sections were mounted on RNase-free Thermo Scientific™ SuperFrost Plus™ slides (J1800AMNZ, Thermo Fisher Scientific, Waltham, MA) for Nissl staining or RNAScope® in situ hybridization. Nissl-stained sections, being parallel to thick sections, guided precise HVC localization for microdissection. All sections were stored at −80°C until further processing.

2.7 | Measurement of the HVC volume

Thin serial sections (20 or 14 μm) were Nissl-stained for HVC volume measurement. Sections were sequentially hydrated through an ethanol series (100%, 90%, 70%, 20% ethanol and distilled water, each for 50–60 s), stained with 0.1% thionine solution for 5–8 s, and then dehydrated (distilled water, 20%, 70%, 90%, and 100% ethanol, each for 30 s). Finally, slides were cleared in xylene and covered with Roti-Histokitt II embedding medium (Roth).

HVC areas were measured using the ImageJ2 (Fiji distribution).[48,49] All brains were coded to ensure blinded evaluation. Volumes were calculated from summed-area measurements multiplied by section thickness and spacing. While section thickness varied between some samples (40 vs. 50 μm), we did not observe systematic differences in HVC volume measurements related to section thickness within experimental groups. However, we acknowledge this variation as a potential confounding factor in our analysis. The Nissl-stained sections of one T3d bird were of poor quality, so its HVC volume was not measured. See Table 1 for sample sizes.

2.8 | RNAScope® in situ hybridization assay

We performed RNAScope® in situ hybridization for *AR* and *SRD5A2* mRNA expression on 20- or 14-μm-thick sections using the RNAScope® 2.0 HD Detection Kit (Advanced Cell Diagnostics, Newark, CA), following the manufacturer's protocols.[50] Three birds were used per probe at each time point, with three slices per bird. Probe details are summarized in Supplemental Table 9. Stained sections were imaged using a Leica DM6000 B microscope and quantified with ImageJ2. Chromogenic particles in the HVC were measured and normalized to the HVC area. The Color Threshold function (RGB; red: 0–47, green: 0–165, blue: 0–160) and Analyze Particles function (minimum size: 8 μm^2) were used to count and measure particle areas. User-defined macro files are available on GitHub (https://github.com/maggieMCKO/TimeLapseTestoFemaleCanary/blob/ce9261d1cf96e760351733657434e499dea35174/RNAscopeQuantification/Marco_quantify_density_singleProbes_quantify_area.ijm).

2.9 | Microarray procedures and annotation

Forty-two adult female canaries (six birds per group) were planned for microarray analysis following the method proposed by.[51] However, three birds were excluded due to insufficient RNA, resulting in 39 canaries being used (see Table 1). The procedure was described in.[52]

We extracted total RNA by dissecting the HVC from 40 or 50 μm sections under a stereomicroscope, referencing adjacent Nissl-stained sections. The HVC is located ventral to the hippocampus, lateral ventricle, and caudo-dorsal to the lamina mesopallialis in sagittal sections. Approximately 20 slices per HVC were dissected and transferred into an Eppendorf tube with 340 μL of RLT buffer (Qiagen, Valencia, CA). RNA was extracted using the RNeasy® Micro Kit (Qiagen), including a DNase digest step, and assessed for quality using an Agilent 2100 Bioanalyzer and a Nanodrop 1000 spectrometer (Thermo Fisher Scientific). While we acknowledge the differences in thickness as a potential confounding factor for hybridization, we do not expect it to significantly impact our results due to the consistent use of multiple thick sections (approximately 20 slices) for each sample, which should provide sufficient and comparable amounts of RNA across all groups. All samples had RNA integrity numbers (RIN) >7.

Purified RNA samples (≥100 ng) were processed and hybridized using the Ambion WT Expression Kit and the Affymetrix WT Terminal Labeling and Controls Kit (Thermo Fisher Scientific). The cDNA was hybridized to the Custom Affymetrix Gene Chip® MPIO-ZF1s520811 Exon Array.[34,35] Hybridization was performed for 16 h at 45°C and 60 rpm. Arrays were washed, stained, and scanned using the Affymetrix GeneChip Fluidics Station 450 and GeneChip scanner 3000 7G. CEL files were generated with Affymetrix GeneChip Command Console® Software (AGCC), and hybridization quality was assessed using Affymetrix Expression Console™ software.

The custom array included 5.7 million male zebra finch-specific probes corresponding to 25,816 transcripts. Over 90% of transcripts

were annotated to 12,729 human orthologous genes using public (Ensembl, GenBank, UniProt, DAVID)[53–58] and commercial databases (v 21 El Dorado, Genomatix, Precigen Bioinformatics Germany GmbH [PBG], Munich, Germany). The microarray data generated in this study have been deposited in NCBI's Gene Expression Omnibus[59] and are accessible through the GEO Series accession number GSE118522.

This microarray approach was chosen based on its previous successful application in cross-species studies between zebra finches and canaries.[34,35] High-density exon arrays, like the one used in this study, have been shown to be accurate and reliable when using smaller amounts of RNA.[60,61] Given the limited amount of RNA available from our HVC samples (<150 ng), the exon array approach was particularly suitable for our study at the time when we conducted the experiment. While more recent technologies such as RNA-Seq might offer additional advantages, particularly in identifying novel or species-specific transcripts, our microarray platform can detect a substantial proportion (over 80%) of the protein-coding genes in the canary genome,[35] based on the annotation of our probes to human orthologous genes. Furthermore, our approach has proven effective in detecting a large number of differentially expressed genes reported in this study, demonstrating its suitability for addressing our research questions.

2.10 | Analysis of differentially expressed genes

Differential expression analyses were performed using the R package limma,[62] following the workflow of Klaus and Reisenauer.[63] Six pairwise comparisons were conducted using a "paired samples" design (limma user guide, section 9.4), comparing each testosterone-treated group to the control group. Comparisons were corrected for multiple testing using the Benjamini-Hochberg method, with significant differentially expressed transcripts defined by an adjusted p-value <0.05 and a minimum differential expression of |log2(fold change)| ≥ 0.5.

Significantly differentially expressed transcripts were annotated to human orthologous genes. For transcripts from the same gene, average expression was calculated if all transcripts were regulated in the same direction. If both up- and down-regulated transcripts were present, transcripts of the minority direction (<40%) were discarded, and the average expression was calculated from the remaining transcripts (≥60%). Transcripts without human orthologous gene annotation were removed before subsequent analyses. Transcripts were annotated to human orthologous genes to leverage the more comprehensive functional annotations available for human genes, particularly for downstream analyses such as Gene Ontology (GO) term enrichment.

A power analysis was conducted for each probe-set in the pairwise differential expression analysis due to moderate sample sizes. Effect sizes were calculated using robust multichip average (RMA)–normalized expression from CEL files, and power was estimated using the "pwr.t.test" function (two-sided, $\alpha = 0.05$) from the "pwr" R package (v1.3-0).[64] Genes with at least one probe-set having a power ≥0.8 were considered high-power differentially expressed genes. In total, 98% of differentially expressed genes identified by limma with |log2 (fold change)|≥0.5 had a power ≥0.8.

The differential analysis results align with published data at the overlapping time point (T14d; Figure 2E), where elevated mRNA levels of vascular endothelial growth factor receptor (*KDR*) were reported.[28] RNAScope® in situ hybridization assays for androgen receptor (*AR*) and 5α-reductase 2 (*SRD5A2*) confirmed the microarray results (Figure 2).

2.11 | Enrichment analysis of GO terms and KEGG pathways

We used the "enrichGO" and "enrichKEGG" functions of the clusterProfiler v4.12.0 R package[65] to predict the putative biological functions (GO and KEGG) of genes of interest. p values were corrected for multiple comparisons using the Benjamini–Hochberg procedure with an false discovery rate threshold of 0.05, and results were plotted using the R package ggplot2.[66]

2.12 | Experimental design and statistical analysis

All statistical analyses were performed in R.[67] Linear mixed-effect models analyzed fixed effects using the "lme4"[68] and "arm"[69] packages in a Bayesian framework with non-informative priors. Gaussian error distribution was assumed, and model assumptions were verified by visual inspection of residuals. Plasma androgen levels, daily song rate, song length, and syllable repetition rate were log-transformed; normalized stained HVC areas (RNAScope®) were square root transformed. Estimates were simulated 10,000 times using the "sim" function to extract 95% credible intervals (CrI) for the mean of simulated values, representing estimate uncertainty.[70] Effects were considered statistically meaningful if the CrI did not include zero or if the posterior probability of the mean difference was higher than 0.95.[71] Linear mixed-effect models, model estimates, and posterior probabilities are detailed in Supplemental Tables 2 and 3. Predicted estimates, 2.5% and 97.5% CrI, and raw data were plotted for visualization. Statistically meaningful differences are inferred if one group's CrI does not overlap with the mean estimate of the other group.

2.13 | Material availability statement

The datasets presented in this study are available in online repositories. Microarray CEL files can be accessed on NCBI's Gene Expression Omnibus GSE118522. The custom MATLAB sound analysis program, MCA, is available on GitLab https://doi.org/10.5281/zenodo.1489098. Processed microarray data, plasma androgen levels, HVC volume measurements, and song parameters are deposited on Dryad. All analysis and visualization scripts are available on GitHub https://github.com/maggieMCKO/TimeLapseTestoFemaleCanary.

3 | RESULTS

3.1 | Testosterone implantation acutely and persistently elevated plasma testosterone levels

Testosterone implants increased plasma androgen levels in all treated groups (Figure 1B, Supplemental Tables 2, and 3). Pre-implantation levels were statistically similar across groups (159 ± 449 pg/mL, mean ± SD). Implantation increased plasma androgen levels by at least 28-fold above baseline (range: 17 to 88 ng/mL) after 1 h, with no significant differences between testosterone-treated groups post-implantation (CON 0.0472 ± 0.0240; T1h 46.9 ± 28.2; T3h 53.9 ± 14.8; T8h 35.6 ± 24.0; T3d 20.4 ± 4.47; T7d 14.8 ± 3.29; T14d 9.31 ± 2.94 ng/mL).

3.2 | Testosterone-induced song development

We selected non-singing females to establish a homogeneous baseline for testosterone-induced song development. Song activity was monitored post-hormone implantation to determine the timing of testosterone-induced vocalization (Figure 1).

Birds in groups T1h, T3h, T8h, and T3d either called or remained silent post-implantation, while five of six birds in group T7d and all birds in group T14d sang (Figure 1, Supplemental Figure 1, and Supplemental Table 1). Careful examination of recordings from all groups confirmed that only T7d and T14d birds developed vocalizations meeting our criteria for songs. The first recognizable subsongs, characterized as unstructured, low-amplitude vocalizations consisting of three or more syllables, were uttered 4.1 ± 1.6 (mean ± SD) days after implantation. This timing aligns with previous reports in female canaries[33] and is comparable to observations in testosterone-implanted male canaries during the non-breeding season.[72] Notably, one female in the T14d group sang just 1 day post-treatment.

Given that only T7d and T14d groups had sufficient time to develop song-like vocalizations, song data analysis was limited to these groups. For the first 7 d, data from T7d and T14d birds were combined as their songs did not differ significantly during this period (Supplemental Figure 3, Supplemental Tables 2, and 3). Singing activity showed two significant increases: first after day 2, and then again after day 10 of testosterone treatment. Between days 2 and 9, singing activity remained relatively stable with no statistically significant changes (Figure 1C, Supplemental Tables 2, and 3).

3.3 | Progressive song development

Songs produced in the early stages of testosterone-induced song development (including subsong and early plastic song) displayed substantial inter- and intra-individual variability (Figure 1, Supplemental Figure 2, and Supplemental Table 1). We observed a gradual increase in song length and complexity over time. Testosterone significantly increased song lengths daily until day 7 and again from day 11 onwards (Figure 1D, Supplemental Tables 2, and 3). Similarly, the number of syllables per song increased daily post-implantation (Figure 1E).

Testosterone implantation significantly increased the syllable repetition rate in two distinct steps: initially on day 2 and subsequently on day 9 (Figure 1F). The maximum observed syllable repetition rate was 26 Hz, consistent with previous findings.[73]

3.4 | Testosterone increased HVC volume after 2 weeks

HVC volumes were significantly larger in T14d birds compared to controls (Figure 1G, CON: 0.103 ± 0.040 mm^3; T14d: 0.253 ± 0.087 mm^3, mean ± SD; Kruskal–Wallis followed by Dunn post hoc test, $\chi^2 = 16.15$, df = 6, Holm-adjusted p-value = 0.013). HVC volumes in T7d birds (0.146 ± 0.073 mm^3) did not significantly differ from controls (Holm-adjusted p-value = 1) or T14d birds (Holm-adjusted p-value = 0.69), likely due to high variability in the T7d group.

Testosterone treatment did not significantly affect body weight, brain weight, or oviduct weight (Figure 1; Supplemental Figure 4A–C). HVC volumes normalized to brain weight yielded similar results as non-normalized volumes (Kruskal–Wallis test, $\chi^2 = 17.32$, df = 6, p-value = 0.0082, Figure 1; Supplemental Figure 4D).

These findings align with previous studies demonstrating that systemic testosterone administration leads to increased HVC volumes in female canaries.[29–32,73,74]

3.5 | Testosterone dramatically alters HVC transcriptomes

To investigate testosterone's effect on gene regulation in the HVC, we performed microarray analyses on the six testosterone-treated groups and controls. Testosterone's impact on transcription was evident as early as 1 h post-implantation (T1h; Figure 2A), coinciding with significantly elevated plasma androgen levels (Figure 1; see Methods). Given our moderate sample sizes, we conducted a power analysis for each differentially expressed gene, considering only genes with power ≥0.8 (Figure 2; Supplemental Figure 1).

At T1h, 2739 genes showed significant differential expression compared to controls: 861 upregulated and 1878 downregulated, including 118 upregulated and 151 downregulated transcription factors (TFs) (Figure 2A, Figure 2–Supplemental Figure 1A, and Supplemental Table 4). The number of differentially expressed genes fluctuated during testosterone treatment, with the most dramatic increase observed at our final time point of 14 days (T14d; Figure 2A). At T14d, 5223 genes were upregulated and 3628 downregulated, including 446 upregulated and 322 downregulated TFs. These 8851 genes represent 57% of all known protein-coding genes (15,609) in the canary genome.[35] Across all time points, testosterone treatment affected the expression of 9913 genes, corresponding to approximately 64% of all canary protein-coding genes.

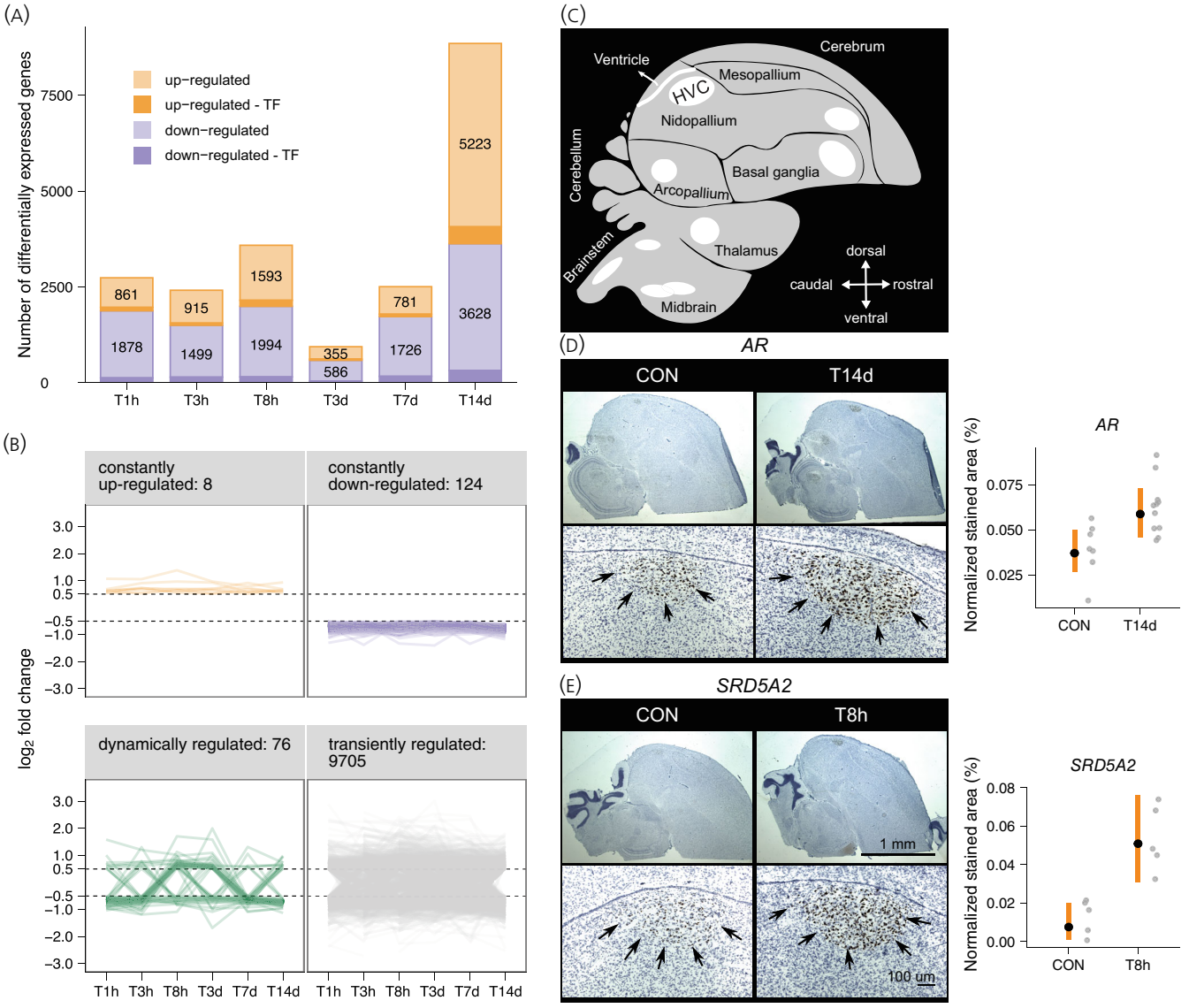

FIGURE 2 Testosterone rapidly and persistently altered gene expression patterns in the HVC. (A), number of differentially expressed genes in the HVC of testosterone-treated birds compared to controls. Darker shades indicate transcription factors (TF). Within 1 h (T1h), over 2700 genes were differentially regulated, with a substantial increase at 14 days (T14d). (B), classification of differentially expressed genes based on temporal regulation patterns: (1) constantly upregulated, (2) constantly downregulated, (3) dynamically regulated, and (4) transiently regulated genes (see Supplemental Table 5). (C), schematic of songbird brain with song control areas (white) including the HVC. (D and E), testosterone increased expression of androgen receptor (*AR*) and 5α-reductase (*SRD5A2*) mRNA in the HVC. Representative RNAScope® in situ hybridization images were shown for *AR* mRNA (D) and *SRD5A2* mRNA (E) in controls (CON) and testosterone-treated birds (T14d and T8h, respectively). Arrowheads indicate increased expression in treated birds. Quantification confirms microarray-derived expression differences (see Figure 3A, Supplemental Tables 2, and 3). Data represent the proportion of labeled HVC area relative to total HVC area. Gray dots: Individual section values; Black dots: Predicted estimates from linear mixed-effects models; Orange bars: 95% confidence intervals (CrI). $N = 3$ birds per group.

3.6 | The vast majority of testosterone-induced genes are only transiently affected

To understand the temporal dynamics of testosterone-altered gene expression, we classified differentially expressed genes into four categories: (1) constantly upregulated (at all six time points), (2) constantly downregulated, (3) dynamically regulated (direction of regulation varied between time points), and (4) transiently regulated (altered expression at least at one but not all time points) (Figure 2B). Contrary to our expectation of a gradual increase in affected genes over time, we observed a rapid and massive impact characterized by a dynamic, nonlinear pattern. The majority of differentially expressed genes (9705) were transiently regulated, while only 208 genes fell into the constant-regulated classes combined (Figure 2B). Further analysis of

the transient category revealed that 45% (4338) of these genes were differentially regulated at just one time point (Figure 2; Supplemental Figure 1C).

Constantly upregulated genes included *KIF5C* (kinesin Family Member 5C) and *NCAM1* (neural cell adhesion molecule 1). *KIF5C* mutations are associated with cortical malformations and

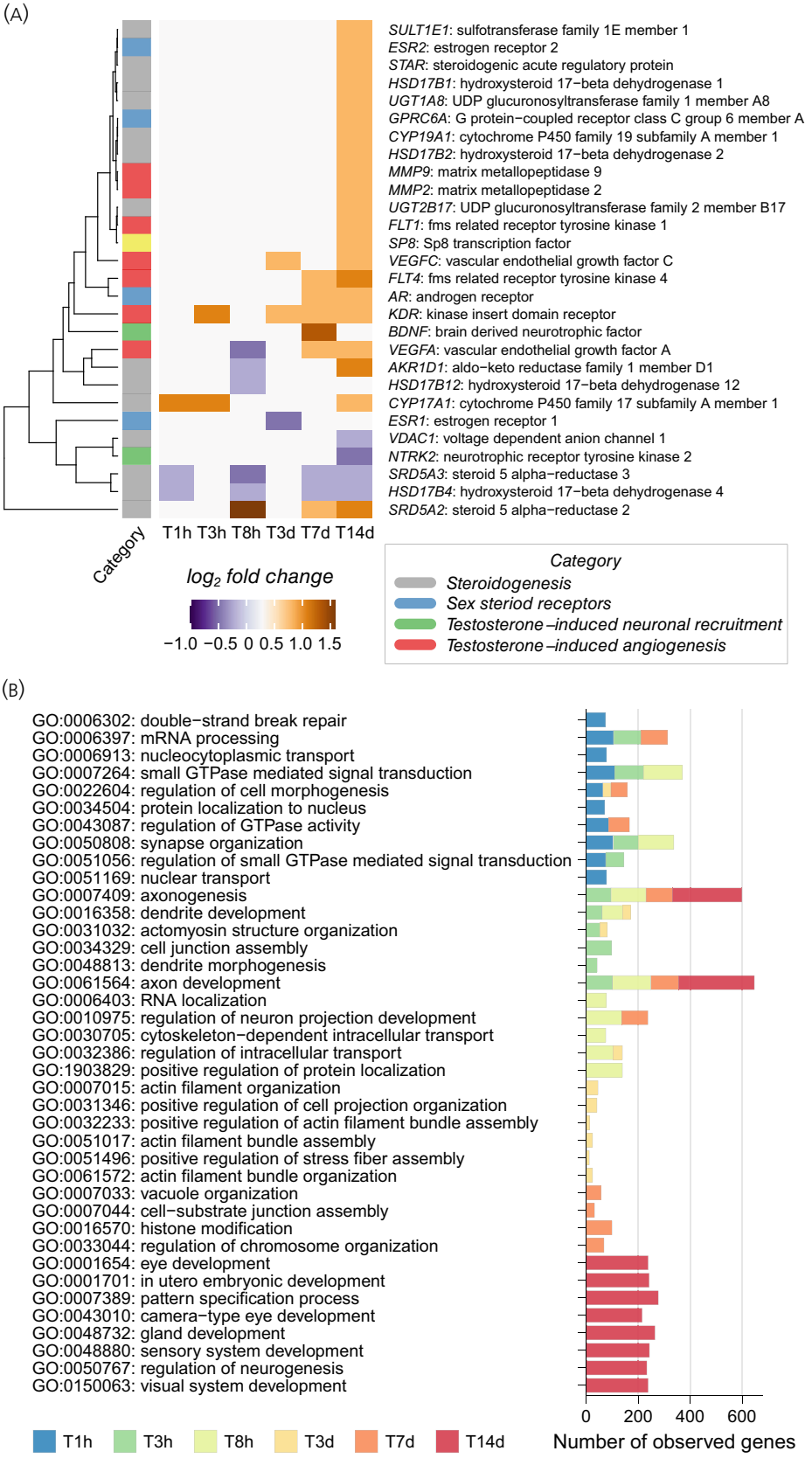

FIGURE 3 Temporal dynamics of testosterone-induced gene regulation in the HVC. A, dendrogram showing expression levels of selected gene groups during testosterone treatment compared to control HVCs (log_2 fold change). Groups include gonadal steroid receptor genes (blue), steroidogenesis genes (gray), testosterone-induced angiogenesis genes (red), and neuronal recruitment genes (green). See Figure 3 – Supplemental 1 for bird-level normalized expression levels of *AR*, *SRD5A2*, *ESR1*, and *ESR2*. B, GO term enrichment analysis of biological processes involving differentially expressed genes during progressive testosterone action on the HVC. The top 10 most significant GO terms (based on Benjamini-Hochberg P-values) are displayed for each time point. The stacked bar graph shows a cumulative number of genes observed across time points (see Supplemental Table 6 for full results). Biological processes at cellular levels occur early (1 h), while organ/system level processes emerge later (14 days).

microcephaly,[75] while *NCAM1* is involved in various brain processes, including neurite growth, axonal and dendritic elongation, and neuronal migration[76] (Supplemental Table 5).

Among the constantly downregulated genes, several were associated with synapse organization and function, including *PSEN1* (presenilin 1), *TSC2* (tuberous sclerosis complex 2), *VPS35* (vacuolar protein sorting 35), *CAMK2G* (calcium/calmodulin dependent protein kinase II gamma), and the serotonin receptor *HTR2C* (5-hydroxytryptamine receptor 2C) (Supplemental Table 5).

3.7 | Testosterone induces dynamic changes in steroidogenesis, hormone metabolism, and vascularization genes

Microarray results revealed significant changes in genes involved in steroidogenesis, hormone metabolism, and vascularization, with distinct temporal dynamics observed across various time points post-testosterone implantation (Figure 3A).

Steroidogenesis and hormone metabolism genes showed marked changes. At the early time point of 1 h, *CYP17A1* (cytochrome P450 17A1) was upregulated, while *HSD17B4* (hydroxysteroid 17-beta dehydrogenase 4) and *SRD5A3* (steroid 5 alpha-reductase 3) were downregulated. By 8 h, *SRD5A2* (5α-reductase type 2) was upregulated, while *AKR1D1* (aldo-keto reductase family 1 member D1) and *HSD17B12* (hydroxysteroid 17-beta dehydrogenase 12) were downregulated. At 14 days, *CYP17A1*, *CYP19A1* (aromatase), *SRD5A2*, *AKR1D1*, *UGT1A8*, and *UGT2B17* were upregulated.

Steroid receptors also exhibited significant changes. The *AR* was upregulated at 7 and 14 days, suggesting increased androgen sensitivity. Estrogen receptors showed dynamic regulation, with *ESR1* (estrogen receptor 1) downregulated at 3 days and *ESR2* (estrogen receptor 2) upregulated at 14 days. *GPRC6A*, a potential membrane AR, was upregulated at 14 days.

Vascularization-related genes also showed significant changes. *KDR* (kinase insert domain receptor) was upregulated at multiple time points from 3 h to 14 days (except T8h), while *VEGFC* (vascular endothelial growth factor C) showed upregulation at later time points. Other vascularization genes, including *FLT4*, *FLT1*, and *VEGFA*, exhibited dynamic regulation patterns across the treatment period.

These changes in mRNA expression suggest complex effects of testosterone on the neural and vascular environment in the HVC. The differential regulation of genes involved in steroidogenesis and vascularization suggests that testosterone may influence both hormone metabolism and vascular support, potentially enhancing neural function and plasticity. The dynamic regulation of androgen and estrogen receptors further underscores the complexity of hormone-driven gene regulation in the brain. Further studies are necessary to confirm these findings and elucidate the mechanisms underlying these gene expression changes.

3.8 | Testosterone-induced genes are first associated with cellular changes and later with neural system changes

GO term enrichment analysis was performed to predict potential biological processes affected by testosterone implantation in the HVC at different time points (Figure 3B and Supplemental Table 6). One hour after testosterone treatment, genes associated with processes such as synapse organization (GO:0050808) and regulation of cell morphogenesis (GO:0022604) were enriched. By 3 h, genes related to neural projections, including axon development (GO:0061564) and dendrite development (GO:0016358), showed enrichment. Many processes associated with cellular anatomical changes demonstrated continuous enrichment from T1h to T14d. KEGG pathway enrichment analysis yielded similar findings (Figure 3, Supplemental Figure 2A, and Supplemental Table 7).

At T14d, the biological processes of differentially expressed genes shifted dramatically. Alongside earlier active processes associated with cellular differentiation, broader functions such as organ formation and system development emerged, including in utero embryonic development (GO:0001701) and sensory system development (GO:0048880). Additional GO term enrichment analysis of 3269 genes differentially regulated only at T14d also revealed mainly system-level processes (Figure 3, Supplement Figure 2B, and Supplemental Table 8). These observations suggest significant changes throughout the entire HVC after approximately 14 days of testosterone treatment.

These findings indicate that testosterone treatment initially influences cellular and morphological processes in the HVC, progressively leading to broader systemic and neural developmental changes over time, culminating in significant alterations after 14 days. This temporal progression underscores the complex interplay between hormonal regulation and gene expression in orchestrating structural and functional transformations in the HVC.

4 | DISCUSSION

Our study reveals unprecedented transcriptomic plasticity in the adult brain, demonstrating how hormonal signals can rapidly and extensively remodel neural circuits underlying complex learned behaviors (Figure 4). By examining testosterone-induced song development in female canaries, we uncovered a dynamic gene regulatory landscape in the HVC, a key song control nucleus. The rapid structural changes we observe under testosterone treatment alone mirror previous findings of HVC plasticity in birds exposed to both long days and testosterone.[77,78] This comparison highlights testosterone's ability to drive rapid neural reorganization independently of photoperiodic state.

The temporal dynamics of gene expression in the HVC following testosterone treatment were striking. Within 1 h of testosterone exposure, 2739 genes exhibited differential expression in the HVC, preceding any observable changes in song behavior. This number

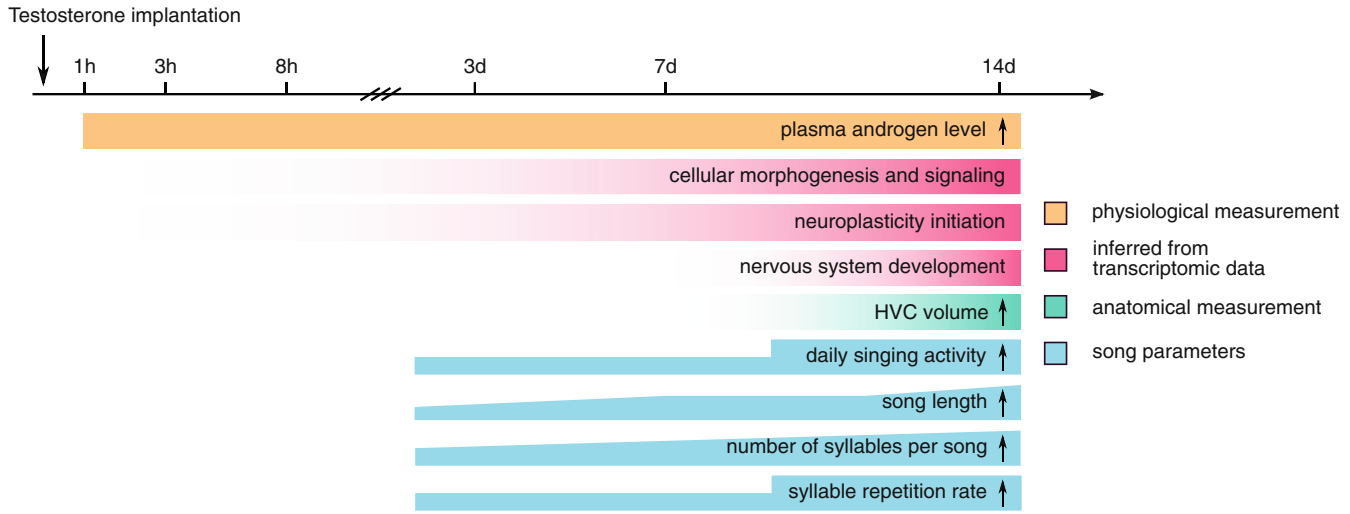

FIGURE 4 Timeline of HVC differentiation and song development following testosterone treatment. This figure illustrates the temporal progression of HVC organizational levels derived from transcriptome data, HVC morphology measured as volume, and song activity and syntax measurements after testosterone treatment. The intensities of colors indicate the abundance or prominence of features. Biological processes related to the circulatory system and neuron development precede those associated with the nervous system development of HVC and the emergence of song. The appearance of canary-typical song patterns coincides with the system development of HVC. HVC morphology (volume) reaches maturity only after approximately 2 weeks of treatment, coinciding with the most differentiated song patterns uttered by the canaries. This timeline provides a comprehensive view of the parallel developments in gene expression, neuroanatomy, and behavior throughout the testosterone-induced song-learning process.

escalated to 8851 genes by day 14, coinciding with the emergence of male-like song patterns. Remarkably, over 98% of the 9913 differentially expressed genes were regulated at specific time points, suggesting that distinct developmental stages require unique transcriptional networks.

The temporal specificity of gene regulation closely mirrored the progression of song development. Early transcriptional changes (T1h to T3d) are primarily related to neuronal and cellular differentiation, potentially priming the HVC for initial vocalizations. As birds advanced to producing plastic songs around T7d, we observed enrichment in genes associated with neuronal differentiation and BDNF signaling, known to regulate the recruitment and survival of adult-born neurons.[79] The most extensive transcriptional changes occurred at T14d, correlating with significant HVC enlargement and the production of near-crystallized songs.

The dramatic shift in gene expression at T14d is particularly noteworthy. Alongside earlier active processes associated with cellular differentiation, broader functions such as organ formation and system development emerged. This suggests that testosterone-induced song development involves a restructuring of the entire HVC, reminiscent of embryonic developmental processes. This parallel between adult plasticity and embryonic development provides intriguing insights into the mechanisms of hormone-induced behavioral changes in adults.

The scale of gene regulation observed in this study far exceeds previous reports in CNS literature, which typically identify fewer than 2000 differentially expressed genes.[14,15,80–90] This discrepancy may be attributed to the high expression of androgen and estrogen receptors in HVC neurons[22,23,91,92] and the cellular diversity of the HVC.[93] However, we cannot exclude the possibility that species-specific factors, methodological variations, and the extended duration of our study also contributed to these differences. Moreover, the striking parallels between late-stage (T14d) gene expression patterns and those observed in embryonic organ formation suggest that testosterone may trigger adult behaviors through extensive transcriptomic restructuring of relevant brain areas. It is important to note that the testosterone implants used in this study induced circulating testosterone levels significantly higher than those typically observed in reproductively active males or spontaneously singing females. This may have implications for the interpretation of our transcriptomic data. In our previous study,[52] we compared the transcriptomes between spontaneously singing female canaries with naturally elevated plasma androgen levels and females induced to sing by testosterone implants. We observed more differentially expressed genes in testosterone-induced singing females than in spontaneously singing females, suggesting that supraphysiological hormone levels may indeed affect gene expression patterns beyond physiological responses.

The observed difference in circulating testosterone levels between early (3 h) and later time points (7 and 14 d) may reflect the pharmacokinetics of our implant system. Despite the decline from the initial peak, testosterone remained significantly elevated throughout the study, potentially maintaining physiological effects. The release mechanism of the implant and the resulting plasma testosterone profile may influence the patterns of gene expression observed. While this variability is a limitation of our study, the sustained elevation above baseline supports the validity of our findings. Future studies could explore various testosterone doses and alternative delivery methods to achieve more constant hormone levels, helping to differentiate between physiological and potential pharmacological effects

on gene expression and clarifying the relationship between testosterone concentrations and gene expression changes over time. Our findings raise intriguing questions about the mechanisms underlying this remarkable neural plasticity. The rapid onset of transcriptional changes suggests direct regulation by androgen and estrogen receptors, while the subsequent waves of gene expression likely involve complex cascades of secondary effectors. The extensive remodeling of the HVC transcriptome may reflect not only changes in neuronal gene expression but also alterations in glial and vascular components,[28–30,32,33] contributing to the observed increase in HVC volume.

While our study focused on the HVC, singing involves a broader song control system.[18] Future research should investigate testosterone's effects on other brain areas within this system to provide a more comprehensive understanding of the neural basis of singing behavior. Additionally, disentangling the direct effects of testosterone from those induced by increased singing activity presents an important challenge for future studies, as singing itself can influence gene expression in the HVC.[94–97]

In conclusion, our results demonstrate that adult song development involves a series of precisely timed, large-scale transcriptional events that reshape the entire HVC. This work provides unprecedented insights into the molecular underpinnings of hormone-induced neural plasticity and lays the groundwork for future studies exploring the relationship between gene regulation and complex behavioral outputs in the adult brain. Furthermore, it highlights the remarkable ability of the adult brain to undergo extensive, orchestrated changes in response to hormonal signals, reminiscent of developmental processes typically associated with embryonic stages.

AUTHOR CONTRIBUTIONS

Meng-Ching Ko: Conceptualization; methodology; software; investigation; formal analysis; project administration; visualization; writing – original draft; writing – review and editing; data curation. **Carolina Frankl-Vilches:** Formal analysis; supervision; methodology; writing – review and editing. **Antje Bakker:** Methodology; investigation. **Nina Sohnius-Wilhelmi:** Investigation; methodology. **Pepe Alcami:** Formal analysis; investigation; writing – review and editing. **Manfred Gahr:** Conceptualization; funding acquisition; project administration; writing – review and editing; writing – original draft; supervision; resources; formal analysis.

ACKNOWLEDGMENTS

We thank Dr. Stefan Leitner for providing breeding canaries, Roswitha Brighton and David Witkowski for maintaining the colony, and Dr. Wolfgang Goymann and Monika Trappschuh for conducting the radioimmunoassay of plasma androgens. We also appreciate the valuable comments on previous versions of this manuscript from Drs. Maude Baldwin, Falk Dittrich, Vincent Van Meir, and Michiel Vellema. Additionally, we acknowledge the support and training provided by the International Max Planck Research School for Organismal Biology. Open Access funding enabled and organized by Projekt DEAL.

CONFLICT OF INTEREST STATEMENT

The authors declare no conflicts of interest.

PEER REVIEW

The peer review history for this article is available at https://www.webofscience.com/api/gateway/wos/peer-review/10.1111/jne.13476.

DATA AVAILABILITY STATEMENT

The data that support the findings of this study are available in Dryad at https://datadryad.org/stash/dataset/doi:10.5061/dryad.5hqbzkh8c, reference number 5hqbzkh8c. These data were derived from the following resources available in the public domain: Omnibus, https://www.ncbi.nlm.nih.gov/geo/query/acc.cgi?acc=GSE118522.

ORCID

Meng-Ching Ko https://orcid.org/0000-0002-2234-9380

REFERENCES

1. Riters LV, Baillien M, Eens M, et al. Seasonal variation in androgen-metabolizing enzymes in the diencephalon and telencephalon of the male European Starling (Sturnus vulgaris). *J Neuroendocrinol*. 2001;13:985-997.
2. Riters LV, Eens M, Pinxten R, Duffy DL, Balthazart J, Ball GF. Seasonal changes in courtship song and the medial preoptic area in male European starlings (Sturnus vulgaris). *Horm Behav*. 2000;38:250-261.
3. Watts HE. Seasonal regulation of behaviour: what role do hormone receptors play? *Proc Biol Sci*. 2020;287:20200722.
4. Ball GF, Balthazart J. Neuroendocrine mechanisms regulating reproductive cycles and reproductive behavior in birds. *Hormones, Brain and Behavior* Elsevier. 2002;12:649-798.
5. Guh Y-J, Tamai TK, Yoshimura T. The underlying mechanisms of vertebrate seasonal reproduction. *Proc Jpn Acad Ser B Phys Biol Sci*. 2019;95:343-357.
6. Gahr M. Where is the asexual brain? *Horm Behav*. 2004;46:130.
7. Apfelbeck B, Kiefer S, Mortega KG, Goymann W, Kipper S. Testosterone affects song modulation during simulated territorial intrusions in male black redstarts (Phoenicurus ochruros). *PLoS One*. 2012;7:e52009.
8. Gahr M. Seasonal hormone fluctuations song structure birds. In: Aubin T, Mathevon N, eds. *Coding Strategies Vertebrate Acoustic Communication*. Vol. 7. 2020;163-201.
9. Alliende J, Giret N, Pidoux L, del Negro C, Leblois A. Seasonal plasticity of song behavior relies on motor and syntactic variability induced by a basal ganglia–forebrain circuit. *Neuroscience*. 2017;359:49-68.
10. Ball GF, Auger CJ, Bernard DJ, et al. Seasonal plasticity in the song control system: multiple brain sites of steroid hormone action and the importance of variation in song behavior. *Ann N Y Acad Sci*. 2004;1016:586-610.
11. Celec P, Ostatníková D, Hodosy J. On the effects of testosterone on brain behavioral functions. *Front Neurosci*. 2015;9:12.
12. Fuentes N, Silveyra P. Estrogen receptor signaling mechanisms. *Adv Protein Chem Struct Biol*. 2019;116:135-170.
13. Balthazart J, Choleris E, Remage-Healey L. Steroids and the brain: 50 years of research, conceptual shifts and the ascent of non-classical and membrane-initiated actions. *Horm Behav*. 2018;99:1-8.
14. Bao R, Onishi KG, Tolla E, et al. Genome sequencing and transcriptome analyses of the Siberian hamster hypothalamus identify mechanisms for seasonal energy balance. *Proc Natl Acad Sci U S A*. 2019;116:13116-13121.
15. Peterson MP, Rosvall KA, Choi JH, et al. Testosterone affects neural gene expression differently in male and female juncos: a role for

hormones in mediating sexual dimorphism and conflict. *PLoS One*. 2013;8:e61784.
16. Nottebohm F, Nottebohm ME, Crane L. Developmental and seasonal changes in canary song and their relation to changes in the anatomy of song-control nuclei. *Behav Neural Biol*. 1986;46:445-471.
17. Voigt C, Leitner S. Seasonality in song behaviour revisited: seasonal and annual variants and invariants in the song of the domesticated canary (Serinus canaria). *Horm Behav*. 2008;54:373-378.
18. Wild JM. Functional neuroanatomy of the sensorimotor control of singing. *Ann N Y Acad Sci*. 2004;1016:438-462.
19. Gahr M. How hormone-sensitive are bird songs and what are the underlying mechanisms? *Acta Acust United Acust*. 2014;100:705-718.
20. Alcami P, Totagera S, Sohnius-Wilhelmi N, et al. Extensive GJD2 expression in the song motor pathway reveals the extent of electrical synapses in the songbird brain. *Biology (Basel)*. 2021;10:1099.
21. Nottebohm F, Stokes TM, Leonard CM. Central control of song in the canary, Serinus canarius. *J Comp Neurol*. 1976;165:457-486.
22. Gahr M. Localization of androgen receptors and estrogen receptors in the same cells of the songbird brain. *Proc Natl Acad Sci U S A*. 1990; 87:9445-9448.
23. Johnson F, Bottjer SW. Differential estrogen accumulation among populations of projection neurons in the higher vocal center of male canaries. *J Neurobiol*. 1995;26:87-108.
24. Hahnloser RHR, Kozhevnikov AA, Fee MS. An ultra-sparse code underliesthe generation of neural sequences in a songbird. *Nature*. 2002;419:65-70.
25. Long MA, Fee MS. Using temperature to analyse temporal dynamics in the songbird motor pathway. *Nature*. 2008;456:189-194.
26. Frankl-Vilches C, Gahr M. Androgen and estrogen sensitivity of bird song: a comparative view on gene regulatory levels. *J Comp Physiol A Neuroethol Sens Neural Behav Physiol*. 2018;113-126. doi:10.1007/s00359-017-1236-y
27. Gahr M. Distribution of sex steroid hormone receptors in the avian brain: functional implications for neural sex differences and sexual behaviors. *Microsc Res Tech*. 2001;55:1-11.
28. Louissaint A, Rao S, Leventhal C, et al. Coordinated interaction of neurogenesis and angiogenesis in the adult songbird brain. *Neuron*. 2002;34:945-960.
29. Rasika S, Nottebohm F, Alvarez-Buylla A. Testosterone increases the recruitment and/or survival of new high vocal center neurons in adult female canaries. *Proc Natl Acad Sci U S A*. 1994;91:7854-7858.
30. Nottebohm F. Testosterone triggers growth of brain vocal control nuclei in adult female canaries. *Brain Res*. 1980;189:429-436.
31. Madison FN, Rouse ML Jr, Balthazart J, Ball GF. Reversing song behavior phenotype: testosterone driven induction of singing and measures of song quality in adult male and female canaries (Serinus canaria). *Gen Comp Endocrinol*. 2015;215:61-75.
32. Hartog TE, Dittrich F, Pieneman AW, et al. Brain-derived neurotrophic factor signaling in the HVC is required for testosterone-induced song of female canaries. *J Neurosci*. 2009;29:15511-15519.
33. Vellema M, Diales Rocha M, Bascones S, et al. Accelerated redevelopment of vocal skills is preceded by lasting reorganization of the song motor circuitry. *elife*. 2019;8:e43194. doi:10.7554/eLife.43194
34. Dittrich F, Ramenda C, Grillitsch D, et al. Regulatory mechanisms of testosterone-stimulated song in the sensorimotor nucleus HVC of female songbirds. *BMC Neurosci*. 2014;15:1-16.
35. Frankl-Vilches C, Kuhl H, Werber M, et al. Using the canary genome to decipher the evolution of hormone-sensitive gene regulation in seasonal singing birds. *Genome Biol*. 2015;16:19.
36. Larson TA, Lent KL, Bammler TK, et al. Network analysis of microRNA and mRNA seasonal dynamics in a highly plastic sensorimotor neural circuit. *BMC Genomics*. 2015;16:905.
37. Thompson CK, Meitzen J, Replogle K, et al. Seasonal changes in patterns of gene expression in avian song control brain regions. *PLoS One*. 2012;7:e35119.
38. Alcami P, Ma S, Gahr M. Telemetry reveals rapid duel-driven song plasticity in a naturalistic social environment. *bioRxiv*. 2021; 803411.
39. Kilkenny C, Browne WJ, Cuthill IC, Emerson M, Altman DG. Improving bioscience research reporting: the ARRIVE guidelines for reporting animal research. *PLoS Biol*. 2010;8:e1000412.
40. Griffiths R, Double MC, Orr K, et al. A DNA test to sex most birds. *Mol Ecol*. 1998;7:1071-1075.
41. Ko M-C, van Meir V, Vellema M, et al. Characteristics of song, brain-anatomy and blood androgen levels in spontaneously singing female canaries. *Horm Behav*. 2020;117:104614.
42. Tchernichovski O, Nottebohm F, Ho CE, Pesaran B, Mitra PP. A procedure for an automated measurement of song similarity. *Anim Behav*. 2000;59:1167-1176.
43. Gardner M. White and brown music, fractal curves and one-over-f fluctuations.
44. Gisiger T. Scale invariance in biology: coincidence or footprint of a universal mechanism? *Biol Rev Camb Philos Soc*. 2001;76:161-209.
45. Voss RF, Clarke J. '1/f noise' in music and speech. *Nature*. 1975;258: 317-318.
46. Wingfield JC, Smith JP, Farner DS. Endocrine responses of White-crowned sparrows to environmental stress. *Condor*. 1982;84: 399-409.
47. Goymann W, Möstl E, Gwinner E. Non-invasive methods to measure androgen metabolites in excrements of European stonechats, Saxicola torquata rubicola. *Gen Comp Endocrinol*. 2002;129:80-87.
48. Rueden CT, Schindelin J, Hiner MC, et al. ImageJ2: ImageJ for the next generation of scientific image data. *BMC Bioinformatics*. 2017; 18:529.
49. Schindelin J, Arganda-Carreras I, Frise E, et al. Fiji: an open-source platform for biological-image analysis. *Nat Methods*. 2012;9:676-682.
50. Wang F, Flanagan J, Su N, et al. RNAscope: a novel in situ RNA analysis platform for formalin-fixed, paraffin-embedded tissues. *J Mol Diagn*. 2012;14:22-29.
51. Pan W, Lin J, Le CT. How many replicates of arrays are required to detect gene expression changes in microarray experiments? A mixture model approach. *Genome Biol*. 2002;3:research0022.
52. Ko M-C, Frankl-Vilches C, Bakker A, Gahr M. The gene expression profile of the song control nucleus HVC shows sex specificity, hormone responsiveness, and species specificity among songbirds. *Front Neurosci*. 2021;15:680530.
53. Yates A, Akanni W, Amode MR, et al. Ensembl 2016. *Nucleic Acids Res*. 2016;44:D710-D716.
54. Benson DA, Karsch-Mizrachi I, Lipman DJ, et al. GenBank. *Nucleic Acids Res*. 2005;33:D34-D38.
55. The UniProt Consortium. UniProt: a hub for protein information. *Nucleic Acids Res*. 2015;43:D204-D212.
56. Flicek P, Amode MR, Barrell D, et al. Ensembl 2014. *Nucleic Acids Res*. 2014;42:D749-D755.
57. Huang DW, Sherman BT, Lempicki RA. Systematic and integrative analysis of large gene lists using DAVID bioinformatics resources. *Nat Protoc*. 2008;4:44-57.
58. Huang DW, Sherman BT, Lempicki RA. Bioinformatics enrichment tools: paths toward the comprehensive functional analysis of large gene lists. *Nucleic Acids Res*. 2009;37:1-13.
59. Edgar R, Domrachev M, Lash AE. Gene expression omnibus: NCBI gene expression and hybridization array data repository. *Nucleic Acids Res*. 2002;30:207-210.
60. Xu W, Seok J, Mindrinos MN, et al. Human transcriptome array for high-throughput clinical studies. *Proc Natl Acad Sci U S A*. 2011;108: 3707-3712.
61. Raghavachari N, Barb J, Yang Y, et al. A systematic comparison and evaluation of high density exon arrays and RNA-seq technology used to unravel the peripheral blood transcriptome of sickle cell disease. *BMC Med Genet*. 2012;5:28.

62. Ritchie ME, Phipson B, Wu D, et al. Limma powers differential expression analyses for RNA-sequencing and microarray studies. *Nucleic Acids Res*. 2015;43:e47.
63. Klaus B, Reisenauer S. An end to end workflow for differential gene expression using Affymetrix microarrays. *F1000Res*. 2016;5:1384.
64. Champely S. Pwr: Basic Functions for Power Analysis. https://CRAN.R-project.org/package=pwr (2020, Accessed July 3, 2024)
65. Wu T, Hu E, Xu S, et al. clusterProfiler 4.0: a universal enrichment tool for interpreting omics data. *Innovation (Camb)*. 2021;2:100141.
66. Wickham H. *ggplot2: Elegant Graphics Data Analysis*. Springer-Verlag; 2016.
67. R Core Team. R: A Language and Environment for Statistical Computing. https://www.R-project.org/ 2024.
68. Bates D, Mächler M, Bolker B, Walker S. Fitting linear mixed-effects models Usinglme4. *J Stat Softw*. 2015;67:1-48.
69. Gelman A, Su Y-S. arm: Data Analysis Using Regression and Multilevel/Hierarchical Models. https://CRAN.R-project.org/package=arm 2024.
70. Gelman A, Hill J. *Data analysis using regression and multilevel/hierarchical models*. Cambridge University Press, 2006.
71. Korner-Nievergelt F, Roth T, von Felten S, et al. Normal linear models. *Bayesian Data Analysis Ecology Using Linear Models R, BUGS, Stan*. Academic Press; 2015.
72. Sartor JJ, Ball GF. Social suppression of song is associated with a reduction in volume of a song-control nucleus in European starlings (Sturnus vulgaris). *Behav Neurosci*. 2005;119:233-244.
73. Fusani L, Metzdorf R, Hutchison JB, Gahr M. Aromatase inhibition affects testosterone-induced masculinization of song and the neural song system in female canaries. *J Neurobiol*. 2003;54:370-379.
74. Cornez G, Shevchouk OT, Ghorbanpoor S, Ball GF, Cornil CA, Balthazart J. Testosterone stimulates perineuronal nets development around parvalbumin cells in the adult canary brain in parallel with song crystallization. *Horm Behav*. 2020;119:104643.
75. Poirier K, Lebrun N, Broix L, et al. Mutations in TUBG1, DYNC1H1, KIF5C and KIF2A cause malformations of cortical development and microcephaly. *Nat Genet*. 2013;45:639-647.
76. Parcerisas A, Ortega-Gascó A, Pujadas L, Soriano E. The hidden side of NCAM family: NCAM2, a key cytoskeleton organization molecule regulating multiple neural functions. *Int J Mol Sci*. 2021;22:10021.
77. Thompson CK, Bentley GE, Brenowitz EA. Rapid seasonal-like regression of the adult avian song control system. *Proc Natl Acad Sci U S A*. 2007;104:15520-15525.
78. Tramontin AD, Hartman VN, Brenowitz EA. Breeding conditions induce rapid and sequential growth in adult avian song control circuits: a model of seasonal plasticity in the brain. *J Neurosci*. 2000;20:854-861.
79. Rasika S, Alvarez-Buylla A, Nottebohm F. BDNF mediates the effects of testosterone on the survival of new neurons in an adult brain. *Neuron*. 1999;22:53-62.
80. Bissegger S, Martyniuk CJ, Langlois VS. Transcriptomic profiling in Silurana tropicalis testes exposed to finasteride. *Gen Comp Endocrinol*. 2014;203:137-145.
81. Carrier N, Saland SK, Duclot F, He H, Mercer R, Kabbaj M. The anxiolytic and antidepressant-like effects of testosterone and estrogen in Gonadectomized male rats. *Biol Psychiatry*. 2015;78:259-269.
82. Cheviron ZA, Swanson DL. Comparative Transcriptomics of seasonal phenotypic flexibility in two north American songbirds. *Integr Comp Biol*. 2017;57:1040-1054.
83. Dopico XC, Evangelou M, Ferreira RC, et al. Widespread seasonal gene expression reveals annual differences in human immunity and physiology. *Nat Commun*. 2015;6:7000.
84. Faber-Hammond J, Samanta MP, Whitchurch EA, Manning D, Sisneros JA, Coffin AB. Saccular transcriptome profiles of the seasonal breeding Plainfin midshipman fish (Porichthys notatus), a teleost with divergent sexual phenotypes. *PLoS One*. 2015;10:e0142814.
85. Félix AS, Cardoso SD, Roleira A, Oliveira RF. Forebrain transcriptional response to transient changes in circulating androgens in a cichlid fish. *G3 (Bethesda)*. 2020;10:1971-1982.
86. Morey JS, Neely MG, Lunardi D, et al. RNA-Seq analysis of seasonal and individual variation in blood transcriptomes of healthy managed bottlenose dolphins. *BMC Genomics*. 2016;17:720.
87. Quintela T, Marcelino H, Gonçalves I, Patriarca FM, Santos CRA. Gene expression profiling in the hippocampus of orchidectomized rats. *J Mol Neurosci*. 2015;55:198-205.
88. Sharma A, Das S, Kumar V. Transcriptome-wide changes in testes reveal molecular differences in photoperiod-induced seasonal reproductive life-history states in migratory songbirds. *Mol Reprod Dev*. 2019;86:956-963.
89. Zhang W, Guo Y, Li J, Huang L, Kazitsa EG, Wu H. Transcriptome analysis reveals the genetic basis underlying the seasonal development of keratinized nuptial spines in Leptobrachium boringii. *BMC Genomics*. 2016;17:978.
90. Zhao W, Yuan T, Fu Y, et al. Seasonal differences in the transcriptome profile of the Zhedong white goose (Anser cygnoides) pituitary gland. *Poult Sci*. 2021;100:1154-1166.
91. Gahr M. Delineation of a brain nucleus: comparisons of cytochemical, hodological, and cytoarchitectural views of the song control nucleus HVc of the adult canary. *J Comp Neurol*. 1990;294:30-36.
92. Johnson F, Bottjer SW. Hormone-induced changes in identified cell populations of the higher vocal center in male canaries. *J Neurobiol*. 1993;24:400-418.
93. Colquitt BM, Merullo DP, Konopka G, Roberts TF, Brainard MS. Cellular transcriptomics reveals evolutionary identities of songbird vocal circuits. *Science*. 2021;371:eabd9704.
94. Jarvis ED, Nottebohm F. Motor-driven gene expression. *Proc Natl Acad Sci U S A*. 1997;94:4097-4102.
95. Li X-C, Jarvis ED, Alvarez-Borda B, Lim DA, Nottebohm F. A relationship between behavior, neurotrophin expression, and new neuron survival. *Proc Natl Acad Sci U S A*. 2000;97:8584-8589.
96. Alvarez-Borda B, Nottebohm F. Gonads and singing play separate, additive roles in new neuron recruitment in adult canary brain. *J Neurosci*. 2002;22:8684-8690.
97. Alward BA, Balthazart J, Ball GF. Differential effects of global versus local testosterone on singing behavior and its underlying neural substrate. *Proc Natl Acad Sci U S A*. 2013;110:19573-19578. doi:10.1073/pnas.1311371110

SUPPORTING INFORMATION

Additional supporting information can be found online in the Supporting Information section at the end of this article.

How to cite this article: Ko M-C, Frankl-Vilches C, Bakker A, Sohnius-Wilhelmi N, Alcami P, Gahr M. From silence to song: Testosterone triggers extensive transcriptional changes in the female canary HVC. *J Neuroendocrinol*. 2025;37(6):e13476. doi:10.1111/jne.13476